Metallic state and charge-order metal-insulator transition in the quasi-two-dimensional conductor κ-(BEDT-TTF)$_2$Hg(SCN)$_2$Cl

Natalia Drichko*
Physikalisches Institut, Universität Stuttgart, Pfaffenwaldring 57, 70550 Stuttgart, Germany and Department of Physics and Astronomy, Johns Hopkins University, Baltimore, Maryland 21218, USA

Rebecca Beyer, Eva Rose, and Martin Dressel
Physikalisches Institut, Universität Stuttgart, Pfaffenwaldring 57, 70550 Stuttgart, Germany

John A. Schlueter
Materials Science Division, Argonne National Laboratory, Argonne, Illinois 60439, USA and Division of Materials Research, National Science Foundation, 4201 35 Wilson Boulevard, Arlington, Virginia 2223, USA

S. A. Turunova, E. I. Zhilyaeva, and R. N. Lyubovskaya
Institute of Problems of Chemical Physics, Chernogolovka, Russia

(Received 20 September 2013; revised manuscript received 10 January 2014; published 26 February 2014)

We present a study of optical and dc properties of a highly frustrated organic conductor κ-(BEDT-TTF)$_2$Hg(SCN)$_2$Cl in the 300–10 K temperature range. At temperatures above 30 K, the material shows properties of a half-filled metal with strong electron-electron correlations. At 30 K, the compound undergoes a metal-insulator transition which we identify as a charge-ordering transition. We find that properties of κ-(BEDT-TTF)$_2$Hg(SCN)$_2$Cl are well explained by a model of a paired electron crystal.

DOI: 10.1103/PhysRevB.89.075133 PACS number(s): 71.30.+h, 73.20.Qt, 78.20.−e

I. INTRODUCTION

Electron-electron repulsion is known to give a rise to insulating ground states. Possibilities include Mott insulators with no spatial symmetry breaking and charge-order insulators where the spatial symmetries of the crystalline lattice are broken, as well as strongly correlated metals which can show exotic electronic and magnetic properties [1–3]. An example of the materials where these phenomena are observed are transition-metal oxides and organic conductors. Insulating and metallic ground states of these materials can be understood within the Hubbard model [1]. This model successfully uses a relatively small number of parameters to describe these quite complicated systems. The minimum set of parameters for a Hubbard model on a square lattice is the transfer integrals t and t', frustration rate t'/t, and the strength of electronic correlations. Properties of many systems with a half-filled conductance band can be successfully reproduced by calculations which take only onsite electron correlations U into account, while an extended Hubbard model with both U and intersite repulsion V is necessary in case of quarter-filled compounds [3,4].

The Hubbard model at half-filling for quasi-two-dimensional (quasi-2D) frustrated square lattice has been successfully used [5,6] to describe the phase diagram of organic conductors κ-(BEDT-TTF)$_2$Cu[N(CN)$_2$]X [X= Cl, Br; BEDT-TTF = bis(ethylenedithio)tetrathiafulvalene], named κ-ET-Cu-Cl and κ-ET-Cu-Br later on. Properties of these layered materials are defined by the conducting BEDT-TTF layer, where BEDT-TTF$^{+0.5}$ molecules are organized in dimers, resulting in a quasi-2D lattice with an effectively half-filled band. The ground state changes from the ambient-pressure Mott insulator κ-ET-Cu-Cl ($T_{\mathrm{MI}} \sim 40$ K) [7] to the superconducting metal κ-ET-Cu-Br ($T_c = 11.8$ K) [8–10] on a decrease of effective electronic correlations U/t [11].

A new theoretical approach to dimerized organic conductors with high frustration was recently developed [12,13], motivated by the spin-liquid candidate κ-(BEDT-TTF)$_2$Cu$_2$(CN)$_3$ and the suggestions for ferroelectric behavior [14,15] in this compound. These models address the BEDT-TTF-based dimerized systems by regarding a single BEDT-TTF$^{+0.5}$ as a lattice unit, and thus treating the lattice as quarter-filled with both U and V used as electronic correlation parameters, while taking into account the strong dimerization. As a result of this more sophisticated approach, Refs. [12,13] propose a static or fluctuating charge order within dimers, which can lead to spin-singlet formation.

κ-(BEDT-TTF)$_2$Hg(SCN)$_2$Cl studied here has crystal and electronic structure of the BEDT-TTF conducting layer similar to the compounds discussed above, while the anion layer shows a different chemical composition. This compound shows a larger frustration parameter t'/t and lower U values [16] than the previously studied κ-phase salts, and is a clear example of charge order in a dimerized BEDT-TTF system. We find that in the metallic state above the metal-insulator transition at $T = 30$ K, κ-(BEDT-TTF)$_2$Hg(SCN)$_2$Cl shows optical spectra characteristic of a strongly correlated metal with a half-filled conductance band, which is well understood within a Hubbard model that takes only U into account. Unexpectedly within this approach, the compound undergoes a charge-order metal-insulator transition at 30 K. Thus, our data on κ-(BEDT-TTF)$_2$Hg(SCN)$_2$Cl can be regarded as an experimentally demonstrated limit of the application of the Hubbard model at half-filling to the BEDT-TTF-based dimerized materials. We discuss possible scenarios for the

*Corresponding author: drichko@pha.jhu.edu

metal-insulator transition, and show that the preferred one is a formation of a paired electron crystal [12] with charge order within dimers.

II. EXPERIMENT

The crystals of κ-(BEDT-TTF)$_2$Hg(SCN)$_2$Cl were prepared similarly to the technique described in Ref. [17] by electrocrystallization of BEDT-TTF in the presence of Hg(SCN)$_2$, [Me$_4$N]SCN·KCl, and 8-crown-6 in 1,1,2-trichloroethane at 40 °C temperature and constant current of 0.5 μA. The crystals are platelets with size of about 0.5 × 1.5 × 1.5 mm^3, with the larger face of the crystal corresponding to the conducting (bc) plane.

For single-crystal x-ray diffraction at 300 and 100 K, a black, platelike crystal of κ-(BEDT-TTF)$_2$Hg(SCN)$_2$Cl with dimensions 0.20 × 0.50 × 0.50 mm^3 was glued to the tip of a glass fiber with epoxy and mounted on a Bruker APEX II three-circle diffractometer equipped with an APEX II detector. Temperature control was provided by an Oxford Cryostream 700 Plus Cooler. The data were collected with 0.3° omega scans using MoK_α radiation ($\lambda = 0.710\,73$ Å) with a detector distance of 50 mm. These data collections nominally covered over a hemisphere of reciprocal space by a combination of three sets of exposures; each set had a different phi angle for the crystal with an exposure time of 30 s. Data to a resolution of 0.68 Å were considered in the reduction.

For data collections at 50 and 10 K, a black crystal of approximate dimensions 10 × 10 × 10 μm^3 was attached to a glass fiber with Paratone N oil. Data were collected at the 15ID ChemMatCARS beamline of the Advanced Photon Source at Argonne National Laboratory with a Bruker 6000 CCD detector. Temperature control was achieved through use of a Helijet (Oxford Instruments). The crystal was quenched to 10 K. After an ∼2-h data collection, the temperature was warmed to 50 K at about 5 K/min. The data were collected with 0.5º phi scans using synchrotron radiation ($\lambda = 0.413\,28$ Å) with a detector distance of 60 mm. These data collections nominally covered over a hemisphere of reciprocal space by a combination of two sets of exposures; each set had a different omega angle for the crystal with an exposure time of 0.6 s. Data to a resolution of 0.45 Å were considered in the reduction.

Raw intensity data were corrected for absorption with the program SADABS [18]. The structure was solved and refined using SHELXTL [19]. A direct-method solution was calculated, which provided most of atomic positions from the E-map. Full-matrix least-squares/difference Fourier cycles were performed, which located the remaining atoms. All nonhydrogen atoms, with the exception of the disordered ethylene carbon atoms, were refined with anisotropic displacement parameters. The hydrogen atoms were placed in ideal positions and refined as riding atoms with relative isotropic displacement parameters.

Temperature-dependent dc resistivity measurements were carried out by a four-point technique: 15-μm golden wires were glued to the sample with carbon paste. To reduce cracks, the sample was fixed in a hanging position only held by its four contact wires. To guarantee perfect thermal coupling, the sample was cooled down directly in a bath cryostat with a temperature sensor located close to it. The cooling rate was in the range of 6–20 K per hour; the applied voltage of 200 mV resulted in a current of about 10^{-3} A.

Temperature-dependent reflectivity measurements were carried out using two optical setups. For measurements in the mid-infrared (MIR) range (600–6000 cm^{-1}), we utilized a Bruker 66 IFS equipped with a Hyperon microscope and a Cryovac microcryostat. The reflectivity measurements were done from the best-quality mirrorlike parts of the surface, the absolute values of reflectivity were determined by a comparison with an aluminum mirror. Reflectivity measurements in the far-infrared (FIR) range between 50 and 700 cm^{-1} were performed using a Bruker 113 IFS, and a cold finger Cryovac cryostat. Absolute values of the reflectivity were received by a comparison of the reflectivity of the sample with that of the sample covered with a thin layer of gold [20]. The overlap between the measurements done with these two setups was better than 2%. The crystal axes are oriented according to the room-temperature spectra published in Ref. [21]. From the reflectivity spectra, the optical conductivity was calculated using a Kramers-Kronig analysis. At low frequencies, the data were extrapolated by the Hagen-Rubens relation. The low-frequency extrapolation only very weakly affects the absolute values of conductivity in the measured range. Spectra were extrapolated up to 40 000 cm^{-1} using room-temperature data from Ref. [21], and by a standard extrapolation $R(\omega) \sim (\frac{\omega_0}{\omega})^2$ up to 100 000 cm^{-1}.

III. RESULTS: CRYSTAL STRUCTURE

The crystal structure of κ-(BEDT-TTF)$_2$Hg(SCN)$_2$Cl was originally reported at room temperature in space group Cc [17], but subsequent analysis suggested that the correct space group is $C2/c$ [22]. Herein, we have redetermined the structure in $C2/c$ at 300, 100, 50, and 10 K with substantially improved agreement factors, see Table I [23]. The crystal structure of κ-(BEDT-TTF)$_2$Hg(SCN)$_2$Cl is characterized by alternating layers of BEDT-TTF radical cations and [Hg(SCN)$_2$Cl]$^-$ anions along the crystallographic a axis (see Fig. 1). There is one crystallographically unique BEDT-TTF molecule in the unit cell. As illustrated in Fig. 1(b), the BEDT-TTF molecules pack in a κ-type packing motif [24] that is identified by an orthogonal arrangement of [BEDT-TTF]$_2^+$ dimers. Many $S \ldots S$ intermolecular interactions exist between dimer units. At room temperature, both ethylene end groups are disordered: the group associated with C7/C8 has a 55:45 statistical distribution, while for the C9/C10 group this ratio is 78:22. At 100 K, the configuration of the C9/C10 group is frozen and the C7/C8 conformation is 84% in the staggered conformation. As illustrated in Fig. 1(c), the anionic layer contains polymeric [Hg(SCN)$_2$Cl]$^-$ chains.

IV. RESULTS: OPTICAL PROPERTIES AND dc RESISTIVITY

In Fig. 2, we present reflectivity and conductivity spectra of κ-(BEDT-TTF)$_2$Hg(SCN)$_2$Cl measured along the principal axes ($E \parallel c$ and $E \parallel b$) in the conducting plane at temperatures between 300 and 20 K. The shape of the spectra is very

TABLE I. Crystal data and structure refinement of κ-(BEDT-TTF)$_2$Hg(SCN)$_2$Cl.

Formula	$C_{22}H_{16}ClHgN_2S_{18}$			
M_W	1121.49			
Cryst syst	Monoclinic			
Space group	$C2/c$			
Source	Sealed tube		Synchrotron	
λ (Å)	0.71073		0.41328	
a (Å)	36.5964(9)	36.2617(9)	36.403(5)	36.367(4)
b (Å)	8.2887(2)	8.1222(2)	8.1226(12)	8.1209(9)
c (Å)	11.7503(3)	11.7248(3)	11.7658(17)	11.7410(13)
α (degrees)	90	90	90	90
β (degrees)	90.067(1)	90.266(1)	90.268(2)	90.186(2)
γ (degrees)	90	90	90	90
V (Å^3)	3564.29(15)	3453.21(15)	3478.9(9)	3467.5(7)
Z	4			
D_c (g cm^{-3})	2.090	2.157	2.141	2.248
μ (mm^{-1})	5.472	5.648	1.236	1.240
F (000)	2188			
R (int)	0.0313	0.0316	0.0620	0.0567
Total reflns	31005	21994	70359	69486
Unique reflns	5775	5321	19910	19730
$I > 2\sigma(I)$	5004	5137	17091	18101
$R(F_o), R_w(F_o^2)$[a]	0.0278, 0.0710	0.0207, 0.0538	0.0315, 0.0805	0.0282, 0.0720
T (K)	296(2)	100(2)	50(2)	10(2)

[a] $R(F_o) = \Sigma||F_o| - |F_c||/\Sigma|F_o|, R_w(F_o^2) = [\Sigma(|F_o^2| - |F_c^2|)^2/\Sigma w F_o^2]^{1/2}$.

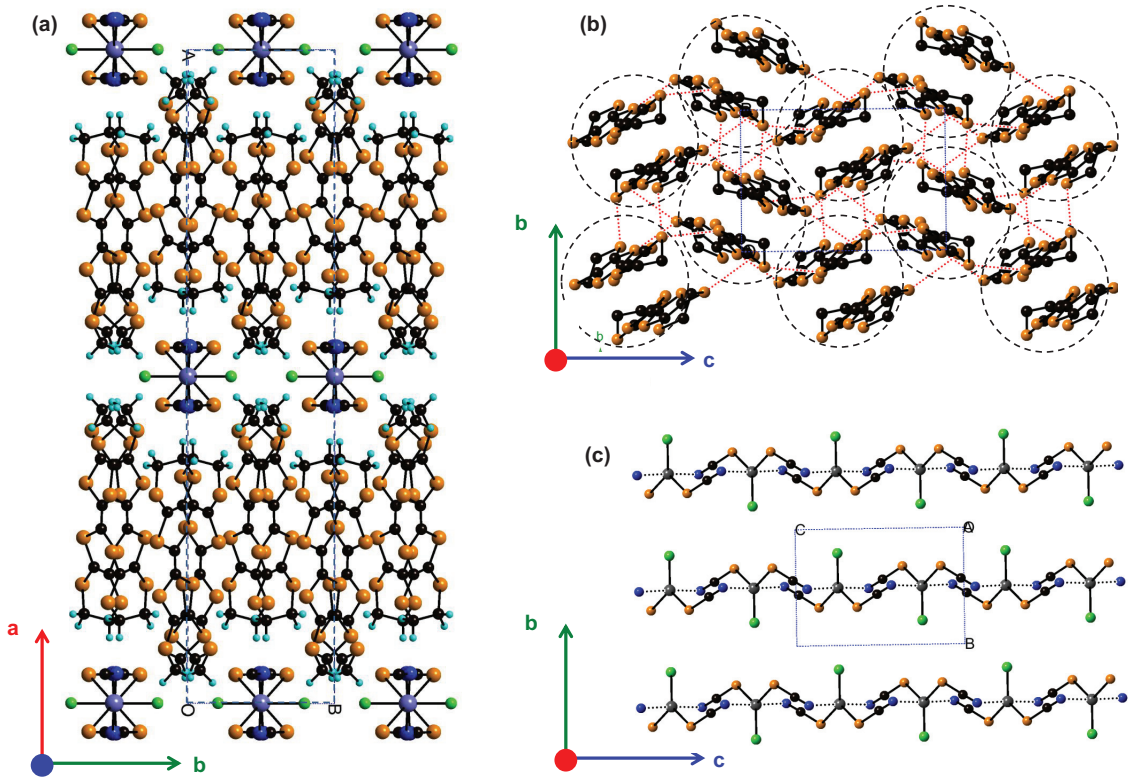

FIG. 1. (Color online) Crystal structure of κ-(BEDT-TTF)$_2$Hg(SCN)$_2$Cl at 100 K. Unit cell borders are marked with a dashed line. (a) Packing diagram illustrating the layered structure along the a axis; (b) Cation BEDT-TTF conducting layer. Dimers $[BEDT\text{-}TT]_2^+$ are marked by circles. Red lines indicate intermolecular $S \ldots S$ interactions less than 3.6 Å. (c) Polymeric anion layer Hg(SCN)$_2$Cl.

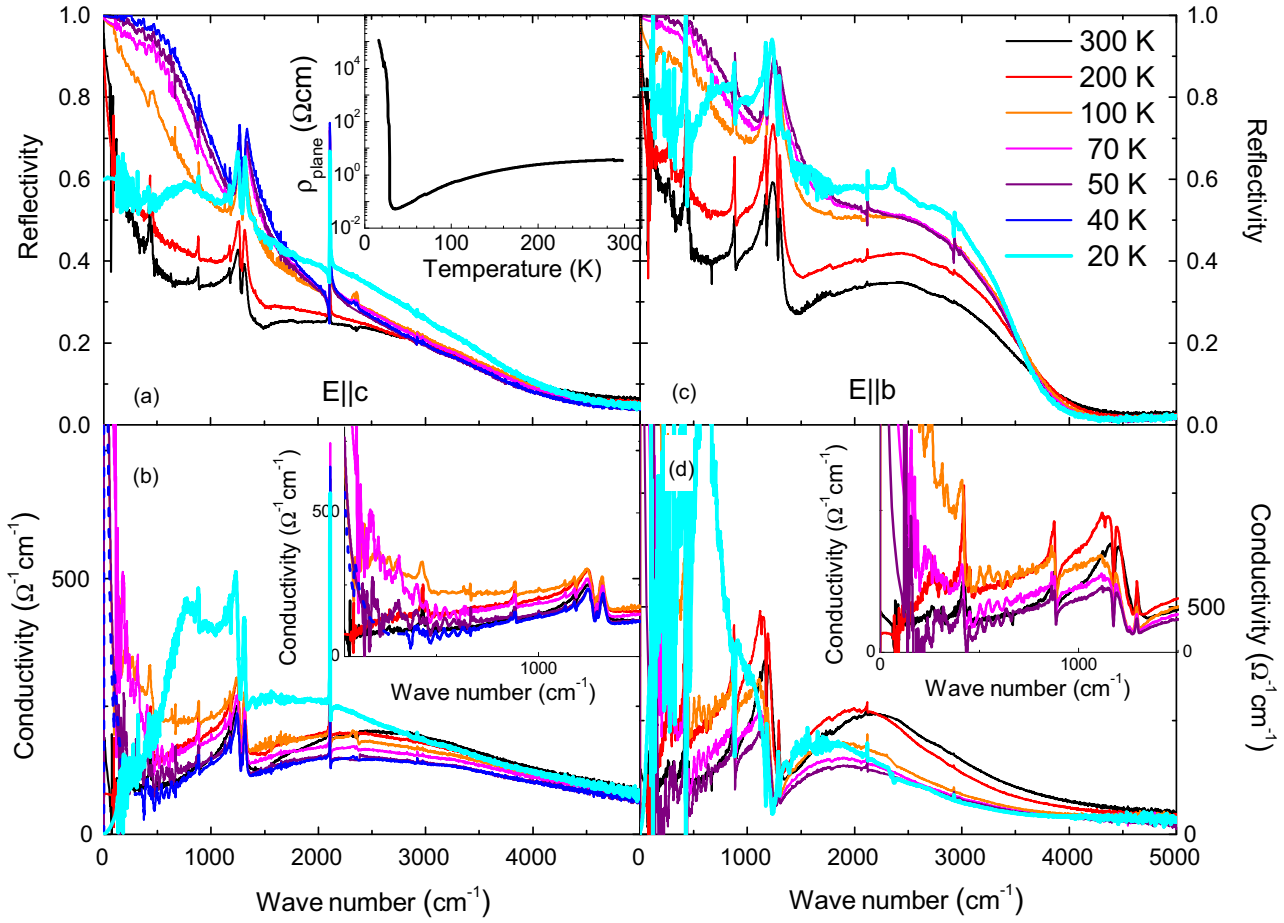

FIG. 2. (Color online) Reflectivity (a), (c) and conductivity (b), (d) spectra of the conducting plane of κ-(BEDT-TTF)$_2$Hg(SCN)$_2$Cl ($E \parallel c$ left panel, $E \parallel b$ right panel) at temperatures between 300 and 20 K. The inset in (a) shows dc resistivity of the κ-(BEDT-TTF)$_2$Hg(SCN)$_2$Cl measured in the conducting plane. The insets in lower panels (b) and (d) show the low-frequency conductivity spectra of the metallic state, where the Drude peak is observed at temperatures between 150 and 40 K.

characteristic for the BEDT-TTF-based κ phases (for example, see Ref. [25] and Fig. 3 of this work). The low-frequency reflectivity and, respectively, conductivity, are relatively low at 300 K. The conductivity spectrum consists of a wide band

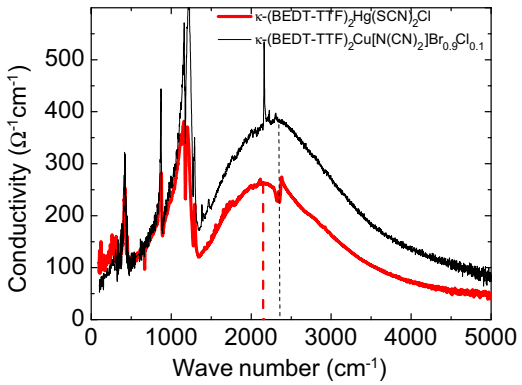

FIG. 3. (Color online) Comparison of the room temperature conductivity spectra of κ-(BEDT-TTF)$_2$Hg(SCN)$_2$Cl, $E \parallel b$ (red line) and κ-(BEDT-TTF)$_2$Cu[N(CN)$_2$]Br$_{0.9}$Cl$_{0.1}$, $E \parallel a$ (black line). The comparison demonstrates that the spectra of the studied compounds are typical for the κ phase.

in the mid-infrared (MIR) range (2200 cm^{-1} for $E \parallel c$ and 2600 cm^{-1} for $E \parallel b$), and intense vibrational features at about 1200 cm^{-1}.

On lowering the temperature from 300 to 30 K, the dc resistivity [Fig. 2(a), inset] shows a metal-like decrease. In agreement with this behavior, the low-frequency reflectivity increases on cooling and, respectively, the spectral weight in the optical conductivity spectra shifts to lower frequencies. At 200 K, the intensity at about 300 cm^{-1} increases while no Drude peak is observed. At 100 K and lower temperatures, we observe a zero-frequency peak in conductivity in both polarizations, corresponding to the response of quasiparticles. At 30 K, the compound undergoes a metal-insulator transition [see Fig. 2(a), inset], with dc resistivity increasing by five orders of magnitude. On this phase transition, the optical spectra change dramatically with reflectivity going down to as low as 0.6 below 1000 cm^{-1}. The optical conductivity spectral weight shifts from the zero-frequency peak to a new maximum at about 700 cm^{-1}. Such a drastic change of the spectrum on the metal-insulator transition is in contrast with the temperature dependence of the spectra on the Mott metal-insulator transition in κ-(BEDT-TTF)$_2$Cu[N(CN)$_2$]Cl where a gradual opening of the Hubbard gap is observed, with a shift of the

spectral weight to the electronic maximum at 2000 cm^{-1} and no new features appearing in the spectra [25].

A. Metallic state

In this section, we will interpret and discuss the spectra of the metallic phase observed above 30 K. The similarity of the κ-(BEDT-TTF)$_2$Hg(SCN)$_2$Cl spectra in the metallic phase to the spectra of the κ-ET-Cu-Cl and κ-ET-Cu-Br (κ-ET-Cu salts) suggests the interpretation of both frequency and temperature dependence of the spectra based on the well-developed picture for κ-ET-Cu salts [10,11,25,26].

Physical properties and, in particular, optical spectra of the κ-ET-Cu family of compounds are well understood within a model that regards the conducting BEDT-TTF layer as a 2D lattice formed by dimers of BEDT-TTF molecules [see Fig. 1(b)]. A dimer is defined as two face-to-face packed BEDT-TTF molecules with a significantly larger transfer integral (t_{dimer}) between them. A simple consideration of a charge of one hole per $[\mathrm{BEDT\text{-}TTF}]_2^+$ lattice site makes such a compound half-filled. Another way to reach the same result is to consider the intrinsic dimerization of the BEDT-TTF conducting layer, which results in a splitting of the $\frac{3}{4}$ conduction band into a full lower band and a half-filled upper band [24].

This model assumes a separation between intradimer and interdimer degrees of freedom. Accordingly, we also expect a separation in energy of intradimer and interdimer transitions in the conductivity spectra [25,27]. The intradimer optical transitions involve a charge transfer between molecules in a dimer. They are observed at about 4000 cm^{-1}(0.5 eV) for κ-ET-Cu salts. Additionally, A_g vibrations of the BEDT-TTF molecule activated by coupling to this electronic transition appear in the spectra as strong Fano-shaped [28] features at around 1200 cm^{-1}. The interdimer phenomena are described in terms of Hubbard model on a 2D frustrated square lattice and the respective charge carriers give origin to the metallic, superconducting, and Mott insulator states. The interdimer optical transitions include the Drude-type response and a transition between lower and upper Hubbard bands, found at about 2500 cm^{-1} (0.4 eV) in a Mott insulator or a metal close to the Mott transition [10,11]. This interpretation of conductivity spectra of κ-ET-Cu salts was recently confirmed by the *ab initio* studies [26].

The conductivity spectra of κ-(BEDT-TTF)$_2$Hg(SCN)$_2$Cl show a broad band in the MIR range (see Fig. 2). It is narrower with a maximum at approximately 2200 cm^{-1} in $E \parallel b$ polarization, and is wider (more damped) with the maximum at higher frequencies, 2600 cm^{-1} in $E \parallel c$ polarization. While the in-plane anisotropy of this MIR band is considerable, it is lower than in the κ-ET-Cu compounds. The large anisotropy of the κ-ET-Cu spectra was explained by the Davydov splitting of the intradimer transitions for the orthorhombic unit cell [25,29]. In the monoclinic κ-(BEDT-TTF)$_2$Hg(SCN)$_2$Cl, the Davydov splitting is absent, and the lower anisotropy of the band due to intradimer transitions prevents us from a clear separation between intradimer and interdimer transitions. Thus, we assign this maximum to the overlapping intradimer transitions, and the transitions between lower and upper Hubbard bands.

Comparing the respective polarization of κ-(BEDT-TTF)$_2$Hg(SCN)$_2$Cl to that of the metal close to the Mott insulator κ-(BEDT-TTF)$_2$Cu[N(CN)$_2$]Br$_{0.9}$Cl$_{0.1}$ at 300 K (Fig. 3), we note that the MIR maximum is observed at about 200 cm^{-1} lower in frequency for κ-(BEDT-TTF)$_2$Hg(SCN)$_2$Cl. The frequency of the transition between lower and upper Hubbard bands is defined by the size of onsite repulsion U (Ref. [11]). The lower values of U in κ-(BEDT-TTF)$_2$Hg(SCN)$_2$Cl (Ref. [16]) can explain the lower frequency of the mid-infrared maximum. In addition, the frequency of the intradimer transition is higher for a closer-packed dimer [30]. The lower values of the transfer integral in a dimer [16] would result in the lower frequencies of the intradimer transition in the studied compound compared to that of κ-ET-Cu salts.

The sharp features at about 1200 cm^{-1} are well studied, and are unambiguously assigned to the A_g vibrations activated by the charge-transfer transition inside the dimer [25,32].

On cooling the sample down to 30 K, the optical spectral weight shifts to lower frequencies, and at temperatures between 100 and 30 K, we observe the zero-frequency peak in the conductivity, giving evidence for a Drude-type coherent carriers response.

1. Coherent charge carriers response

In contrast to the metallic behavior of dc resistivity, at 300 and 200 K the optical conductivity shows low intensity at low frequencies, and the quasiparticle Drude response is overdamped. On cooling down to 200 K we see an increase of intensity at about 500 cm^{-1}[see the insets in Figs. 2(b) and 2(d)]. At temperatures between 100 and 30 K, a zero-frequency peak is observed in the conductivity spectra.

For strongly correlated metals close to the Mott transition, the calculations of optical conductivity within a Hubbard model (see Refs. [3,33]) predict that the coherent charge carriers at high temperatures are destroyed, and a zero-frequency peak in the conductivity spectra appears only below a certain temperature T^*. Indeed, an appearance of the Drude peak only below $T^* = 50$ K was observed for the κ-ET-Cu-Br (see Ref. [25]). κ-(BEDT-TTF)$_2$Hg(SCN)$_2$Cl falls inline with this observation, but the Drude peak appears in the spectra of κ-(BEDT-TTF)$_2$Hg(SCN)$_2$Cl between 200 and 100 K, the increase of T^* correlating with the lower U/t in this compound. In addition, some of the effect of the increased metallicity of the compound can be due to the frustration of the 2D lattice formed by BEDT-TTF dimers [34].

This relatively high T^* allows us to study the temperature dependence of the quasifree charge carrier response. We perform a Drude-Lorentz fit of the spectra above 30 K, fitting simultaneously reflectivity and conductivity spectra; the resulting Drude parameters are shown in Fig. 4. The Drude-Lorentz fit of the spectra suggests that at temperatures above T^*, the wide background which results in nonzero conductivity at zero frequency can be described as an overdamped Drude-type function. However, below 100 K the scattering rate decreases, while the plasma frequency doubles. Since the Drude plasma frequency Ω_p is defined by the spectral weight $\Omega_p^2 = \int \sigma(\omega) d\omega$ [32], we can regard the drastic change in the plasma frequency as reflecting the singularity in the temperature behavior of the density of states on the Fermi level

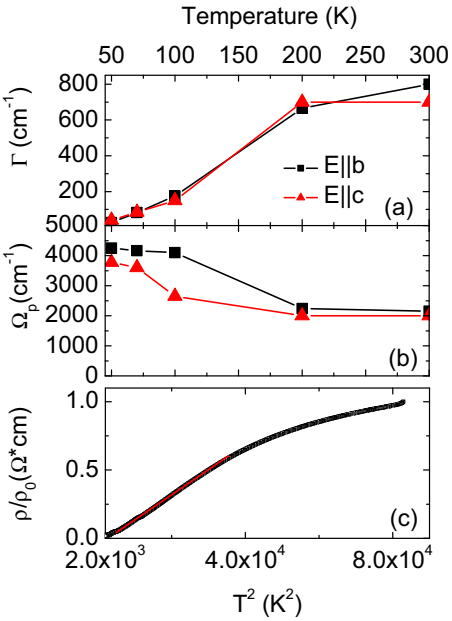

FIG. 4. (Color online) Temperature dependence of the Drude (a) scattering rate Γ and (b) plasma frequency Ω_p determined from a Drude-Lorentz fit of the reflectivity and conductivity spectra of κ-(BEDT-TTF)$_2$Hg(SCN)$_2$Cl. A clear distinction between a high-temperature regime above 150 K, with a weak overdumped Drude response and a Drude-type coherent carriers response below 150 K is observed. Panel (c) shows a resistivity $\rho/\rho_0(T^2)$ dependence. The region between 50 and 170 K follows the T^2 behavior, typical for the Fermi liquid.

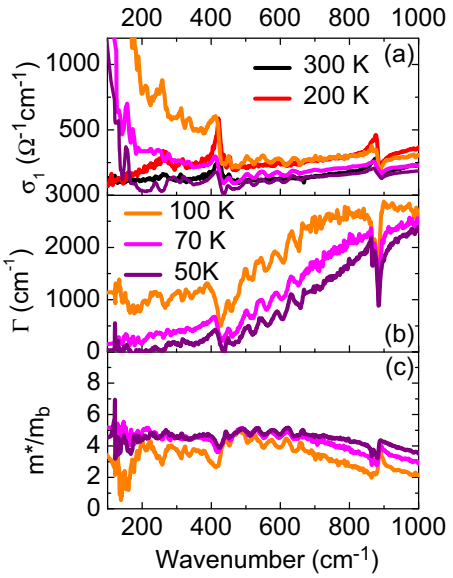

FIG. 5. (Color online) The figure presents (a) optical conductivity spectra of κ-(BEDT-TTF)$_2$Hg(SCN)$_2$Cl in $E \parallel b$ polarization at temperatures between 300 and 50 K in the low-frequency region; (b) frequency-dependent scattering rate $\Gamma_1(\omega)$ at temperatures between 100 and 50 K; and (c) frequency-dependent effective mass of charge carriers m^*/m_b.

[33]. In the coherent regime, the plasma frequency changes only very slightly on cooling, while scattering decreases by an order of magnitude on cooling from 100 to 30 K. A decrease of U/t on cooling suggested by electronic band-structure calculations [16] (see Table II) also can lead to the increase of the Drude plasma frequency. However, the decrease of U/t is gradual from 300 to 50 K, while the Drude parameters exhibit a jump, that shows importance of correlation effects.

The effects of electronic correlations on the renormalization of the effective mass and the lifetime of the coherent charge carriers between 100 and 30 K can be obtained from the extended Drude analysis (for details see Ref. [2] and references therein): $\frac{m^*(\omega)}{m_{b,\mathrm{opt}}} = \frac{\Omega_p^2}{4\pi}\frac{\sigma_2(\omega)/\omega}{|\hat{\sigma}(\omega)|^2}$, $\Gamma_1(\omega) = \frac{\Omega_p^2}{4\pi}\frac{\sigma_1(\omega)}{|\hat{\sigma}(\omega)|^2}$. Here, $\Gamma_1(\omega)$ is the real part of a complex frequency-dependent scattering rate $\hat{\Gamma}(\omega) = \Gamma_1(\omega) + i\Gamma_2(\omega)$, with the imaginary part related to the frequency-dependent enhanced mass (renormalized due to electron-electron interactions) $\frac{m^*(\omega)}{m_{b,\mathrm{opt}}} = 1 - \Gamma_2(\omega)/\omega$.

TABLE II. Parameters of the Hubbard model.

Compound	t'/t	U/t
κ-(BEDT-TTF)$_2$Cu[N(CN)$_2$]Br [31]	0.42	5.1
κ-(BEDT-TTF)$_2$Cu[N(CN)$_2$]Cl [31]	0.44	5.5
κ-(BEDT-TTF)$_2$Cu$_2$(CN)$_3$ [31]	0.83	7.3
κ-(BEDT-TTF)$_2$Hg(SCN)$_2$Cl(300 K) [16]	0.80	5.1
κ-(BEDT-TTF)$_2$Hg(SCN)$_2$Cl (50 K) [16]	0.84	4.37

The results of the analysis are presented in Fig. 5, where the scattering rate and effective mass are calculated using the values of plasma frequencies Ω_p determined from the Drude-Lorentz fit. In the spectral range below 400 cm^{-1}, for temperatures between 100 and 30 K, the Drude peak is the major contribution to the conductivity spectra [Fig. 5(a)]. The frequency dependence of $\frac{m^*(\omega)}{m_{b,\mathrm{opt}}}$ and $\Gamma_1(\omega)$ in this spectral range demonstrates the effects of electronic correlations on charge carriers [Fig. 5(b)]. The values and frequency dependence of both scattering rate and effective mass are close to those received for the more correlated κ-ET-Cu compounds. Indeed, the theoretical calculations for U/t below 10 yield very similar values for $\frac{m^*(\omega)}{m_{b,\mathrm{opt}}}$ and $\Gamma_1(\omega)$ (Ref. [11]).

In the temperature range between 50 and 170 K, where in optical properties we observe a Drude response, the dc resistivity shows a T^2 dependence, indicating the Fermi-liquid behavior [Fig. 4(c)]. In some cases [35,36], a T^2 resistivity dependence can occur due to order-disorder scattering. However, since this behavior is present in the limited temperature range, this is a less possible interpretation. The T^2 dc resistivity behavior is a signature of the electron-electron correlations and is also in agreement with the prediction for electrodynamic properties of half-filled organic conductors [3].

Another effect of the electronic correlations on the temperature dependence of resistivity predicted in Ref. [3] is the maximum at T^*, which was experimentally observed in the dc resistivity curves of metallic κ-ET-Cu compounds. According to the calculations, the intensity of this maximum decreases with U/t and is expected to disappear for the values of $U/t = 2$ at which the materials would show a regular metallic behavior of dc resistivity. While the estimated [16] U/t for the studied compound are between 4 and 5, the dc conductivity of

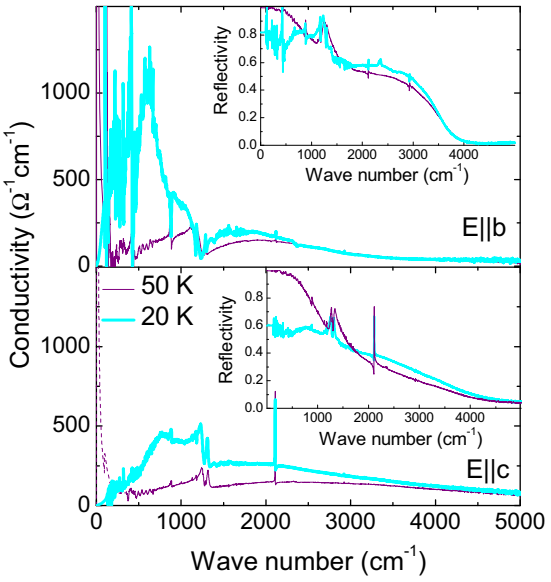

FIG. 6. (Color online) Conductivity spectra of κ-(BEDT-TTF)$_2$Hg(SCN)$_2$Cl above (50 K) and below (20 K) the metal-insulator transition for $E \parallel b$ (upper panel) and $E \parallel c$ (lower panel). The insets show the corresponding reflectivity spectra.

κ-(BEDT-TTF)$_2$Hg(SCN)$_2$Cl shows a smooth decrease with temperature in the metallic phase [Fig. 2(a), inset], reflecting lower influence of electronic correlations.

Summarizing the results for the metallic phase of κ-(BEDT-TTF)$_2$Hg(SCN)$_2$Cl, we see that at temperatures between 300 and 30 K the optical properties give a very consistent picture of a half-filled metallic compound with strong electron-electron correlations. Both frequency and temperature behavior of optical conductivity are in line with the previously reported experimental data for the family of κ-ET-Cu salts [10,11,25], and are in agreement with the calculations on the Hubbard model for a half-filled metal close to the Mott transition. The sharp-metal insulator transition occurring at 30 K is at odds with this approach. Within the Hubbard model that takes into account only onsite electronic correlations U, a metal-insulator transition (MIT) is not expected for the studied compound, which is less correlated than the metallic κ-ET-Cu-Br.

B. Metal-insulator transition

On the metal-insulator transition at 30 K, the dc conductivity increases by a few orders of magnitude, and the spectra in $E \parallel b$ and $E \parallel c$ change drastically (see Fig. 2). At $T = 20$ K, the shape of the conductivity spectra with a U band at about 2000 cm^{-1} is lost, and we observe an optical gap and an intense peak at about 700 cm^{-1}(Fig. 6). A vibrational structure below 700 cm^{-1} can be assigned to the vibrations of BEDT-TTF molecule, that are screened by the response of the quasifree charge carriers in the metallic state. This shape of the spectra is very different to the spectra observed for κ-(BEDT-TTF)$_2$Cu[N(CN)$_2$]Cl in the Mott insulating state [25], suggesting that the ground state of κ-(BEDT-TTF)$_2$Hg(SCN)$_2$Cl is not a Mott insulator.

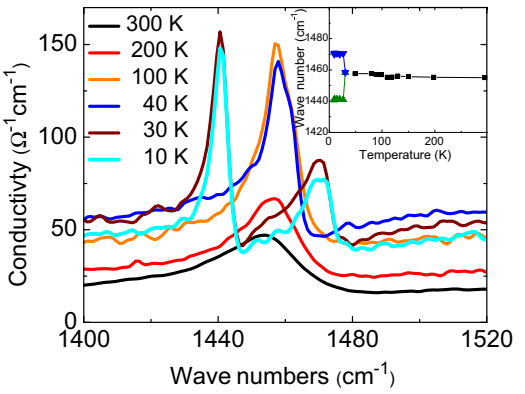

FIG. 7. (Color online) Temperature dependence of the conductivity spectra of κ-(BEDT-TTF)$_2$Hg(SCN)$_2$Cl perpendicular to the conducting plane in the region of $B_{1u}(\nu_{27})$ mode. There is a single mode above 30 K which splits into two components below this temperature. The temperature behavior of the frequency of this vibration is shown in the inset.

1. X-ray structure studies

The x-ray diffraction data at 50 and 10 K were carefully examined for extra reflections that would indicate lattice doubling, but none were found. For the 10-K data, the structure was also solved in the lower symmetry space groups $P2/c$, $P2_1/n$, and $P\bar{1}$ in consideration of whether crystallographically ordered, nonequivalent BEDT-TTF molecules exist in the structure. The agreement factors were poorer in these space groups than in $C2/c$. This is similar to the case of (TMTTF)$_2$SbF$_6$, where single-crystal x-ray diffraction does not indicate a structural transition at the charge-order temperature [37].

2. Charge-order transition demonstrated by vibrational spectroscopy

To investigate the nature of the transition, we performed infrared reflectance measurements in the polarization perpendicular to the conducting layers [$E \perp (bc)$]. In these spectra we observe an insulatorlike optical response, with low reflectivity resulting in low values of conductivity, in agreement with the quasi-2D character of these materials, and previous similar measurements [32]. Superimposed on the low-intensity background are infrared-active (IR) B_{1u} vibrations of the BEDT-TTF molecule and IR lattice vibrations. The frequency dependence of the charge-sensitive $B_{1u}(\nu_{27})$ mode associated with the out-of-phase vibrations of the C=C bonds of inner rings of BEDT-TTF molecule proved to be an efficient method to identify the amount of charge on molecular lattice sites [38,39]. The resulting conductivity spectra in the region of the $B_{1u}(\nu_{27})$ mode are presented in Fig. 7; the temperature dependence of the vibrational frequencies is shown in the inset. The single $B_{1u}(\nu_{27})$ mode is found at 1454 cm^{-1} at room temperature, and becomes narrower on cooling down. While at temperatures below 100 K the single band already shows a double-peak structure, the band splits into two components at 1441 and 1470 cm^{-1} on the metal-insulator transition at 30 K, suggesting that BEDT-TTF molecules with different charges appear below the transition. According to Refs. [38,40], the

difference of 29 cm^{-1} in frequency between the two bands corresponds to two different molecular sites with a charge difference of $0.2e$.

Interestingly, a comparison of room-temperature vibrational spectrum of κ-(BEDT-TTF)$_2$Hg(SCN)$_2$Cl to that of κ-ET-Cu-Br [41] shows that $B_{1u}(\nu_{27})$ is found 10 cm^{-1} lower than the same band in the κ-ET-Cu-Br compound. This can be an evidence of fast charge-order fluctuations [40].

Using the value of charge separation $0.2e$, we can estimate how large will be the relevant change of the central C=C bond length in the BEDT-TTF molecules, which is used in the x-ray analysis to define the charge on a molecule. We use a calculation of a dependence of the C=C bond length for the TTF [42] to estimate the change of the C=C bond length on the charge-order phase transition. Assuming that BEDT-TTF shows a behavior similar to TTF, a change of charge on BEDT-TTF molecule by $0.1e$ would result in the C=C bond changing by about 0.004 Å. A transfer of $0.1e$ would result in $0.4e$ and $0.6e$ charged molecules with a difference of about 0.008 Å in the length of their C=C bond. The measured length of the central C=C bond is 1.3718(12) Å, yielding a resolution limit of about 0.004 Å, which is comparable to the assumed change of the C=C bonds in our case. Indeed, Ref. [43] analyzes BEDT-TTF salts with various charge states and shows that the standard deviation in the charge on BEDT-TTF defined by this method is about $0.1e$. Therefore, while we distinctly observe the charge separation by vibrational spectroscopy, the small value of $0.2e$ charge separation is on the limit of sensitivity for the x-ray structural studies.

3. *Electronic spectra of the insulating phase*

The spectra of the conducting (bc) plane of κ-(BEDT-TTF)$_2$Hg(SCN)$_2$Cl in the insulating state are drastically different from those in the high-temperature metallic phase (Fig. 6). This agrees with the interpretation of the insulating phase as a charge-order insulator, which would introduce essential changes into the electronic structure. In the conductivity spectra we observe an insulating gap of about 100 cm^{-1}, which is approximately an order of magnitude lower compared to the well-studied charge-ordered insulators α-(BEDT-TTF)$_2$I$_3$ [44] and θ-(BEDT-TTF)$_2$RbZn(SCN)$_2$ [45,46].

In the $E \parallel b$ polarization, an intense electronic maximum is observed at 600 cm^{-1}, and the vibrational features at 1200 cm^{-1} have antiresonance shape. This shape is expected within a Fano effect, when the electronic maximum is shifted to the frequencies close to the vibrational features [28,47]. The in-plane anisotropy of the optical spectra increases below the metal-insulator transition. A maximum in conductivity is observed in $E \parallel c$ at 765 cm^{-1}, but shows much lower intensity. The spectra in this direction are reminiscent of the κ-phase metallic state, with the vibrational features at 1200 cm^{-1} showing up as asymmetric peaks.

A mid-infrared maximum is typically observed in the conductivity spectra of quarter-filled BEDT-TTF-based charge-ordered insulators. It is assigned to a charge transfer between a charge-rich and charge-poor site. The theory for a quasi-two-dimensional system with a checkerboard order [48] estimates this maximum to appear at frequencies between V and $2V$ for large values of U. An anisotropy of conductivity spectra of a stripe charge-ordered pattern was suggested by calculations for quasi-two-dimensional quarter-filled BEDT-TTF based θ-phase compounds [45]. Here, for the "vertical stripes" case, a single electronic maximum is expected to have considerably higher intensity in the direction perpendicular to the stripes. The high anisotropy of the spectra in the insulating state of κ-(BEDT-TTF)$_2$Hg(SCN)$_2$Cl suggests that the charge-ordered pattern is anisotropic stripelike, with ordered pattern parallel to the b direction, that would make stripes parallel to the c direction.

A maximum observed in the $E \parallel b$ has an asymmetric shape and lies at lower frequencies compared to the similar electronic response for α [44] or θ [45] phases of BEDT-TTF-based Q2D compounds, where it is typically found in the range of 1500–3000 cm^{-1}. While the charge disproportionation between the sites in κ-(BEDT-TTF)$_2$Hg(SCN)$_2$Cl is relatively small, the maximum is still found at rather low values since an estimate of V for BEDT-TTF-based systems is of 0.5 eV. The maximum has a shape similar to quarter-filled charge-ordered systems with a relatively small gap, for example, 1D charge-ordered insulator δ-(EDT-TTF-CONMe$_2$)$_2$Br [49]. There, the spectrum is interpreted as an optical response of the domain walls in a quarter-filled charge-ordered system, where a single-domain-wall excitation is a charge transition from a charge-rich to a charge-poor site. Indeed, the formation of domain walls is expected in the charge-order organic conductors [45,50,51]. Domain-wall excitations are expected to have an asymmetric line shape, and to be found at lower frequencies of $0.5V$ [52] than a simple transition from a charge-rich to charge-poor site. An interpretation of the electronic maximum in $E \parallel c$ spectra in terms of domain-wall excitations can explain its comparatively low position.

4. *Discussion of the MI transition*

We have shown that the high-temperature metallic state of κ-(BEDT-TTF)$_2$Hg(SCN)$_2$Cl is well understood within a Hubbard model for a half-filled metal close to the Mott insulating state, however, this model does not explain the observed charge-order metal-insulator transition. Thus, we can regard the κ-(BEDT-TTF)$_2$Hg(SCN)$_2$Cl compound as a system which demonstrates both a good agreement with the model and its limitations.

An apparent limit of the application of the Hubbard model at half-filling to the κ-phase salts is an assumption that the conductance layer can be described as a lattice of (BEDT-TTF)$_2^{+1}$ dimers. In a limiting case, if an intradimer transfer integral t_{dimer} will become comparable to an interdimer transfer integral, the dimer description fails. In this case, each BEDT-TTF molecule presents a lattice site with $+0.5e$ charge, the lattice can be well described by an extended Hubbard model with onsite U and intersite V repulsion as parameters. Both charge-ordered insulating and metallic states of quarter-filled BEDT-TTF-based organic conductors were successfully described by this model [4]. A weaker dimerization, 129 meV at 300 K and 117 meV at 50 K compared to approximately 200 meV for the κ-ET-Cu salts [16], makes κ-(BEDT-TTF)$_2$Hg(SCN)$_2$Cl "closer" to a quarter-filled- BEDT-TTF salts.

The structure of κ-(BEDT-TTF)$_2$Hg(SCN)$_2$Cl and, as a result, the values [16] of the transfer integrals do not change

essentially on cooling. A slight change of parameters or temperature effects could introduce a change of the ground state if a compound is close to a phase boundary between the two states. However, a very good agreement of the spectra in the metallic phase with a half-filling model suggests that the dimerization is essential for the properties of this material. The low value of charge disproportionation found in the insulating state ($\delta\rho = 0.2e$) is in contrast with $\delta\rho$ of the well-studied quarter-filled charge-order insulators and points on a possible different mechanism of the insulator transition. For example, θ-(BEDT-TTF)$_2$RbZn(SCN)$_2$ (Refs. [45,46,53]) and α-(BEDT-TTF)$_2$I$_3$ (Refs. [44,54]) show much larger charge disproportionation of $\delta\rho = 0.8e$ and $\delta\rho = 0.6e$, respectively. They have much larger values of the insulating gap in the ordered state, even when structural changes are very small and can be detected only by synchrotron x-ray diffraction, as in case of α-(BEDT-TTF)$_2$I$_3$ (Ref. [55]). At the $\delta\rho = 0.2e$ detected in β''-(BEDT-TTF)$_2$SF$_5$CH$_2$CF$_2$SO$_3$, the metallic state is sustained [39].

It was suggested that a half-filled system can have charge order as a ground state when V is taken into account in the Hubbard model, and U is small compared to V [56]. This would require a creation of two types of dimers within a charge-ordered state, one of which would have both charged molecules $[\text{BEDT-TTF}]_2^{+2}$ and another noncharged $[\text{BEDT-TTF}]_2^0$. This pattern is not probable due to the fact that t_{dimer} is still larger than transfer integrals between the dimers.

Another possibility is to interpret the charge-order phase transition in κ-(BEDT-TTF)$_2$Hg(SCN)$_2$Cl in terms of a paired electronic crystal (PEC) [12,57]. It proposes a possibility for charge ordering in a quarter-filled strongly dimerized system, where an essential parameter of the model is the frustration of the lattice. For correlated systems with low frustration values, a predicted ground state is a dimerized antiferromagnetic state with an equal distribution of charges on the lattice, which can be relevant to κ-ET-Cu-Cl. For certain parameters, including high frustration, a system would undergo a transition to a charge-ordered state at low temperatures, where charge disproportionation is observed between the sites in a dimer. In this ground state, the spins that belong to the neighboring charge-rich sites form a spin singlet, and the bond between these sites gets stronger [57]. A PEC state can occur at charge disproportionation below $\delta\rho_{\text{calc}} = 0.2$, which is also in agreement with a relatively low value of $\delta\rho = 0.2$ we determined from our measurements. This approach would take into account both high- and low-temperature regimes of κ-(BEDT-TTF)$_2$Hg(SCN)$_2$Cl.

In Fig. 8, we show possible patterns of the ordered charge on the orthogonally arranged dimers of the κ-(BEDT-TTF)$_2$Hg(SCN)$_2$Cl structure to see if it can indeed develop the 1100 charge order expected for PEC. Figure 8(a) presents 0101 charge order along the b axis, which results in stripes along the c axis ($P2/c$ symmetry of the unit cell). This possibility is in agreement with the large anisotropy of conductivity in the (bc) plane (see Sec. IV B 3). The arrangements 8(b) show 1010 CO along c and stripes along b ($P2_1/c$ symmetry of the unit cell), and Fig. 8(c) order 1100 along c with stripes along b suggest the anisotropy of conductivity reversed from that observed in the insulating state, and a doubling of the unit cell. Arrangement 8(d) shows 1100 order along both b and c, which would suggest lower anisotropy of the BEDT-TTF layer than the other cases, as well as doubling of the unit cell.

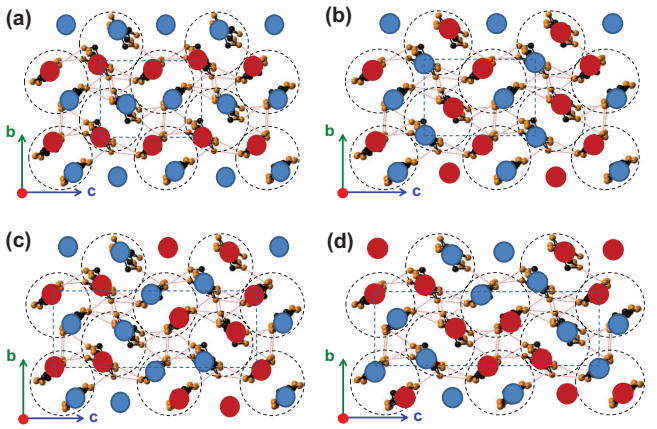

FIG. 8. (Color online) Possible charge-order patterns shown. (a) Shows anisotropy in agreement with the anisotropy of the conductivity spectra ($P2/c$ symmetry of the unit cell); (b) shows anisotropy reversed to that of the conductivity spectra ($P2_1/c$ symmetry of the unit cell); (c), (d) show a doubling of the unit cell and anisotropy lower than observed in the conductivity spectra.

The charge pattern [Fig. 8(a)] basically presents the PEC state proposed for a κ-phase structure in Ref. [57] (see Fig. 4 therein). Since this charge pattern is also in the best agreement with the observed anisotropy of the conductivity spectra, we can consider it as the best explanation of the optical data. Here, we have to note that this charge disproportionation should lower the symmetry of the unit cell from $C2/c$ to $P2/c$. According to a PEC description, the bonds between the charge-rich sites should become shorter as well. As was mentioned in Sec. IV B 1, we do not observe the respective structural change with the x-ray diffraction technique. We showed that the change in the structure due to the charge disproportionation is below the sensitivity of the x-ray diffraction method we were using. Apparently, the changes in bonds are also small and below our detection limit.

Our results for the metallic and charge-order insulating regimes in κ-(BEDT-TTF)$_2$Hg(SCN)$_2$Cl are important in the context of a discussion of the charge-ordered state in the spin-liquid compound κ-(BEDT-TTF)$_2$Cu$_2$(CN)$_3$ (Refs. [13,15]), as well as for antiferromagnetically ordered κ-ET-Cu-Cl (Ref. [14]). The data on κ-(BEDT-TTF)$_2$Hg(SCN)$_2$Cl demonstrate a charge-order state in a κ-phase BEDT-TTF-based frustrated compound, which results in changes of the electronic structure at low frequencies, and is detectable by vibrational spectroscopy. This is in contrast to κ-(BEDT-TTF)$_2$Cu$_2$(CN)$_3$ and κ-ET-Cu-Cl materials, where an absence of charge order was demonstrated by vibrational spectroscopy, and the spectrum at all temperatures is close to that of a κ-phase Mott insulator [41,58].

V. CONCLUSIONS

In this work we present optical, dc resistivity, and structural studies of a strongly correlated organic conductor κ-(BEDT-TTF)$_2$Hg(SCN)$_2$Cl. We show that in the metallic state at temperatures above 30 K, this material demonstrates

properties of a metal with a half-filled conductance band and high-electron correlations. This falls in line with the theoretical studies of half-filled metals close to Mott insulator transition, and the experimental studies of κ-phase half-filled BEDT-TTF-based salts.

Using vibrational spectroscopy, we show that the metal-insulator transition at 30 K is a charge-order transition, which occurs without a detectable structural change. An appearance of this transition demonstrates a limit of applicability of the Hubbard model with only onsite repulsion U to the properties of BEDT-TTF-based κ-phases. We suggest that this charge-order transition can be described within a model of paired electron crystal, which can explain a charge-ordered state in a half-filled dimerized system, with an insulating state at relatively small charge disproportionation. Basing on the experimental conductivity spectra in the insulating state, we propose a charge-order pattern with 1010 order in the b direction and stripes in the c direction in the BEDT-TTF plane, which can be mapped on the 1100 order of parallel dimers proposed for the paired electronic crystal.

Further theory input is necessary to calculate conductivity of the paired electronic crystal to confirm our interpretation. Measurements of magnetic properties of κ-(BEDT-TTF)$_2$Hg(SCN)$_2$Cl, which can confirm a prediction of a spin-singlet state for the PEC, are in progress.

Our finding gives an example of the charge-ordered state in a κ-phase BEDT-TTF-based compound with high frustration and confirms an absence of such order in κ-(BEDT-TTF)$_2$Cu$_2$CN$_3$ and κ-(BEDT-TTF)$_2$Cu[N(CN)$_2$]Cl.

ACKNOWLEDGMENTS

We are grateful to H. Jeschke, R. Valenti, and S. Mazumdar for stimulating discussions, and to H. Jeschke and R. Valenti for providing the unpublished results of their calculations of the electronic structure of κ-(BEDT-TTF)$_2$Hg(SCN)$_2$Cl. N.D. acknowledges support by the Margarete von Wrangell Habilitationstipendium. Work in the University of Stuttgart is supported by by the Deutsche Forschungsgemeinschaft (DFG) via Grant No. DR 228/39-1. Work at JHU was supported by the H. Blewett Fellowship of the American Physical Society and by DOE grant for The Institute of Quantum Matter Grant No. DE-FG02-08ER46544. ChemMatCARS Sector 15 is principally supported by the National Science Foundation/Department of Energy under Grant No. NSF/CHE-0822838. Work at Argonne National Laboratory was supported by the US Department of Energy, Office of Science, Office of Basic Energy Sciences, under Contract No. DE-AC02-06CH11357.

[1] M. Imada, A. Fujimori, and Y. Tokura, Rev. Mod. Phys. **70**, 1039 (1998).
[2] D. N. Basov, R. D. Averitt, D. van der Marel, M. Dressel, and K. Haule, Rev. Mod. Phys. **83**, 471 (2011).
[3] J. Merino and R. H. McKenzie, Phys. Rev. B **61**, 7996 (2000).
[4] J. Merino and R. H. McKenzie, Phys. Rev. Lett. **87**, 237002 (2001).
[5] B. Powell and R. McKenzie, J. Phys.: Condens. Matter **18**, R827 (2006).
[6] N. Toyota, M. Lang, and J. Müller, *Low-Dimensional Molecular Metals*, Vol. 154 (Springer, Berlin, 2007).
[7] S. Yasin, M. Dumm, B. Salameh, P. Batail, C. Meźière, and M. Dressel, Euro. Phys. J. B **79**, 383 (2011).
[8] S. Lefebvre, P. Wzietek, S. Brown, C. Bourbonnais, D. Jérome, C. Méziere, M. Fourmigué, and P. Batail, Phys. Rev. Lett. **85**, 5420 (2000).
[9] F. Kagawa, K. Miyagawa, and K. Kanoda, Nature (London) **436**, 534 (2005).
[10] M. Dumm, D. Faltermeier, N. Drichko, M. Dressel, C. Mézière, and P. Batail, Phys. Rev. B **79**, 195106 (2009).
[11] J. Merino, M. Dumm, N. Drichko, M. Dressel, and R. H. McKenzie, Phys. Rev. Lett. **100**, 086404 (2008).
[12] S. Dayal, R. T. Clay, H. Li, and S. Mazumdar, Phys. Rev. B **83**, 245106 (2011).
[13] C. Hotta, Phys. Rev. B **82**, 241104 (2010).
[14] P. Lunkenheimer, J. Müller, S. Krohns, F. Schrettle, A. Loidl, B. Hartmann, R. Rommel, M. de Souza, C. Hotta, J. A. Schlueter *et al.*, Nat. Mater. **11**, 755 (2012).
[15] M. Abdel-Jawad, I. Terasaki, T. Sasaki, N. Yoneyama, N. Kobayashi, Y. Uesu, and C. Hotta, Phys. Rev. B **82**, 125119 (2010).
[16] H. Jeschke (private communication).
[17] S. V. Konovalikhin, G. V. Shilov, O. A. D'yachenko, R. N. Lyubovskaya, M. Z. Aldoshina, and R. B. Lyubovskii, Bull. of Russ. Acad. Sci.: Phys. **41**, 903 (1992).
[18] G. M. Sheldrick, SADABS, Version 2.03a, Bruker AXS, Inc., Madison, WI, 2001.
[19] G. M. Sheldrick, SHELXTL, Version 6.12, Bruker AXS Inc., Madison, WI, 2001.
[20] C. C. Homes, M. Reedyk, D. A. Cradles, and T. Timusk, Appl. Opt. **32**, 2976 (1993).
[21] R. M. Vlasova, O. O. Drozdova, R. N. Lyubovskaya, and V. N. Semkin, Phys. Solid State **37**, 382 (1995).
[22] R. E. Marsh, Acta Crystallogr., Sect. B: Struct. Sci. **53**, 317 (1997).
[23] A thermal ellipsoid plot at 100 K, illustrating the atom numbering scheme is provided. Crystallographic data for the κ-(BEDT-TTF)$_2$Hg(SCN)$_2$Cl structure at 298, 100, 50, and 10 K has been deposited with the Cambridge Crystallographic Data Centre as Supplementary Publication No. CCDC 956013-956016. Copies of the data can be obtained free of charge on application to CCDC, 12 Union Road, Cambridge CB2 1EZ, UK [fax: (44) 1223 336-033; e-mail: data_request@ccdc. cam.ac.uk].
[24] T. Mori, H. Mori, and S. Tanaka, Bull. Chem. Soc. Jpn. **72**, 179 (1999).
[25] D. Faltermeier, J. Barz, M. Dumm, M. Dressel, N. Drichko, B. Petrov, V. Semkin, R. Vlasova, C. Meźière, and P. Batail, Phys. Rev. B **76**, 165113 (2007).

[26] J. Ferber, K. Foyevtsova, H. O. Jeschke, and R. Valenti, arXiv:1209.4466.
[27] M. Dressel, D. Faltermeier, M. Dumm, N. Drichko, B. Petrov, V. Semkin, R. Vlasova, C. Meziere, and P. Batail, Phys. B (Amsterdam) **404**, 541 (2009).
[28] U. Fano, Phys. Rev. **124**, 1866 (1961).
[29] A. S. Davydov and S. B. Dresner, *Theory of Molecular Excitons*, Vol. 1 (Plenum, New York, 1971).
[30] G. Visentini, M. Masino, C. Bellitto, and A. Girlando, Phys. Rev. B **58**, 9460 (1998).
[31] H. C. Kandpal, I. Opahle, Y.-Z. Zhang, H. O. Jeschke, and R. Valentí, Phys. Rev. Lett. **103**, 067004 (2009).
[32] M. Dressel and N. Drichko, Chem. Rev. **104**, 5689 (2004).
[33] G. Kotliar, E. Lange, and M. J. Rozenberg, Phys. Rev. Lett. **84**, 5180 (2000).
[34] A. Liebsch, H. Ishida, and J. Merino, Phys. Rev. B **79**, 195108 (2009).
[35] M. Gurvitch, Phys. Rev. Lett. **56**, 647 (1986).
[36] M. Dressel, G. Grüner, J. E. Eldridge, and J. M. Williams, Synth. Met. **85**, 1503 (1997).
[37] M. Dressel, M. Dumm, T. Knoblauch, B. Köhler, B. Salameh, and S. Yasin, Adv. Condens. Matter Phys. **2012**, 398721 (2012).
[38] T. Yamamoto, M. Uruichi, K. Yamamoto, K. Yakushi, A. Kawamoto, and H. Taniguchi, J. Phys. Chem. B **109**, 15226 (2005).
[39] S. Kaiser, M. Dressel, Y. Sun, A. Greco, J. A. Schlueter, G. L. Gard, and N. Drichko, Phys. Rev. Lett. **105**, 206402 (2010).
[40] A. Girlando, M. Masino, S. Kaiser, Y. Sun, N. Drichko, M. Dressel, and H. Mori, Phys. Status Solidi B **249**, 953 (2012).
[41] K. Sedlmeier, S. Elsässer, D. Neubauer, R. Beyer, D. Wu, T. Ivek, S. Tomić, J. A. Schlueter, and M. Dressel, Phys. Rev. B **86**, 245103 (2012).
[42] C. Katan, J. Phys. Chem. A **103**, 1407 (1999).
[43] P. Guionneau, C. Kepert, G. Bravic, D. Chasseau, M. Truter, M. Kurmoo, and P. Day, Synth. Met. **86**, 1973 (1997).
[44] T. Ivek, B. Korin-Hamzić, O. Milat, S. Tomić, C. Clauss, N. Drichko, D. Schweitzer, and M. Dressel, Phys. Rev. B **83**, 165128 (2011).
[45] H. Tajima, S. Kyoden, H. Mori, and S. Tanaka, Phys. Rev. B **62**, 9378 (2000).
[46] N. L. Wang, H. Mori, S. Tanaka, J. Dong, and B. P. Clayman, J. Phys.: Condens. Matter **13**, 5463 (2001).
[47] A. Damascelli, K. Schulte, D. van der Marel, and A. A. Menovsky, Phys. Rev. B **55**, R4863 (1997).
[48] J. Merino, A. Greco, R. H. McKenzie, and M. Calandra, Phys. Rev. B **68**, 245121 (2003).
[49] A. Antal, T. Knoblauch, M. Dressel, P. Batail, and N. Drichko, Phys. Rev. B **87**, 075118 (2013).
[50] T. Yamamoto, H. Tajima, J.-I. Yamaura, S. Aonuma, and R. Kato, J. Phys. Soc. Jpn. **68**, 1384 (1999).
[51] S. Fratini and G. Rastelli, Phys. Rev. B **75**, 195103 (2007).
[52] M. Mayr and P. Horsch, Phys. Rev. B **73**, 195103 (2006).
[53] K. Yamamoto, K. Yakushi, K. Miyagawa, K. Kanoda, and A. Kawamoto, Phys. Rev. B **65**, 085110 (2002).
[54] Y. Yue, K. Yamamoto, M. Uruichi, C. Nakano, K. Yakushi, S. Yamada, T. Hiejima, and A. Kawamoto, Phys. Rev. B **82**, 075134 (2010).
[55] T. Kakiuchi, Y. Wakabayashi, H. Sawa, T. Takahashi, and T. Nakamura, arXiv:0708.1696.
[56] A. Hoang and P. Thalmeier, J. Phys.: Condens. Matter **14**, 6639 (2002).
[57] H. Li, R. T. Clay, and S. Mazumdar, J. Phys.: Condens. Matter **22**, 272201 (2010).
[58] S. Elsässer, D. Wu, M. Dressel, and J. A. Schlueter, Phys. Rev. B **86**, 155150 (2012).